Mater. Res. Soc. Symp. Proc. Vol. 841 © 2005 Materials Research Society R12.10.1

A Nanoindentation Study of Thermally-Grown-Oxide Films on Silicon

Fatih Helvaci and Junghyun Cho
Dept. of Mechanical Engineering
Thomas J. Watson School of Engineering
State University of New York
Binghamton, NY 13902, USA

ABSTRACT

We explore the effect of the substrate on mechanical behavior of thin films using a depth-sensing indentation. For this purpose, nanoindentation has been performed on thermally grown silicon oxide films on the silicon substrate. One primary goal of this study is to extract 'film-only' mechanical properties from the nanoindentation data by subtracting the substrate effect. It is also shown that elastic modulus of the film is more influenced by the substrate than hardness due to a larger elastic extension beyond a plastically deformed region, as well as a larger elastic mismatch between the SiO_2 film and the Si substrate. Further, an inverse analysis of indentation data is proposed to estimate a thickness of thin films. Consequently, this study provides a fundamental understanding in mechanical phenomena of thin films occurring at nanoscales.

INTRODUCTION

Thin films have been a key technology in many areas including electronics, magnetic recording media, optical devices, MEMS, and chemical and mechanical protection of engineering components [1]. In such developments, a good understanding of mechanical properties of thin films is essential [2,3]. It is, however, not trivial to evaluate mechanical properties of a thin structural unit of the sub-micron scale by conventional testing methods. Given that, the depth-sensing indentation (nanoindentation) has received great attention as it provides necessary resolution besides its easy adaptation to localized structures [4].

In particular, silicon oxide thin films are of great importance in microelectronics and optics industry [5-7]. For example, the films can be used as inter-level dielectrics and gate dielectrics in metal-oxide-semiconductor field effect transistors (MOSFETs) and thin films transistors (TFTs), protective layers in metallic mirrors, anti-reflection coatings, and low index layers in multilayer coatings for the mid-IR range [8-13].

Although nanoindentation is an excellent tool, a good interpretation of the indentation data is important to have reliable and repeatable results for mechanical behavior of thin films. In addition, influence of substrates often makes it difficult to establish 'film-only' mechanical properties. Previously it was reported that 10-25% of the film thickness would be a proper range for indentation to avoid the substrate effect [14]. It will be therefore challenging to do nanoindentation on ultrathin films since the indentation will be performed beyond this range.

Numerous models have been developed in order to obtain true thin film properties from nanoindentation data [14]. Accurate determination of the reduced modulus and projected contact area prior to application of the nanoindentation models would be critical. One purpose of this study is then to characterize the SiO_2 thin films grown on the Si substrates while assessing the substrate effect.

EXPERIMENTAL DETAILS

The testing specimens were cut from a wafer of the n-type (100) Si single crystal (Silicon Quest International, Santa Clara, CA). The SiO_2 films were thermally grown on the Si substrates by annealing at 1000˚C (with a 10˚C/min ramp) in air with different time durations. Four SiO_2 films were prepared with different thicknesses, which were measured by ellipsometry: 53-nm (annealed for 100 sec), 88-nm (1,000 sec), 293-nm (10,000 sec), 370-nm (100,000 sec).

All the nanoindentation measurements were performed using the TriboScope Nanoindenter (Hysitron Inc., Minneapolis, MN) with a Berkovich tip. The attached AFM unit provided *in-situ* topography images. Multiple indentations (3 or more) were made at each load, with the data presented here representing the average value of the group.

In nanoindentation, hardness (H) and modulus (E) are routinely obtained by having a measurement of the elastic contact stiffness (S) and the projected contact area (A). In this study, the contact stiffness was obtained by fitting the upper portion (20 to 95% of the maximum load) of the unloading data. The projected contact area was calculated by evaluating an empirical area function of the indenter used,

$$A = f(h_c) \quad , \tag{1}$$

where h_c is the contact depth determined from an analysis of the indentation load-displacement data,

$$h_c = h_{\max} - \varepsilon \frac{P_{\max}}{S} \quad , \tag{2}$$

where h_{max} is a maximum displacement and ε a geometric constant ($\varepsilon = 0.75$ for Berkovich indenter).

The hardness (H) and modulus (E) are derived from the contact stiffness, S and projected contact area, A. Joslin and Oliver [15] first suggested a parameter P/S^2 while eliminating the projected contact area,

$$\frac{P}{S^2} = \frac{1}{\beta^2}\frac{\pi}{4}\frac{H}{E_r^2} \quad , \tag{3}$$

where P is load and β is a dimensionless parameter that depends on the geometry of the indenter [16]. $\beta = 1.05$ was chosen for the Berkovich tip [17]. This P/S^2 parameter is independent of the indenter tip shape calibration and penetration depth, and should be constant throughout the depth of indentation, provided that the material is homogenous [15]. Once the true hardness is known, the reduced modulus at a specific displacement can be obtained

$$E_r = \sqrt{\frac{1}{\beta^2}\frac{\pi}{4}\frac{1}{(P/S^2)}H} \quad . \tag{4}$$

Also, the projected contact area, A can be given by

$$A = \frac{1}{\beta^2}\frac{\pi}{4}\left(\frac{S}{E_r}\right)^2 \quad . \tag{5}$$

In this study, we explore the dependence of the indentation depth on hardness and modulus of thin oxide films, and utilize the model to determine the true thin film properties.

RESULTS AND DISCUSSION

The load-displacement curves consisting of two parts, loading and unloading, for the SiO_2 films are shown in Fig. 1. Among the four films, pop-in effects (sudden increase in a displacement) are observed for the first two short annealed films at the loading curve that have been annealed for 100 sec and 1000 sec.

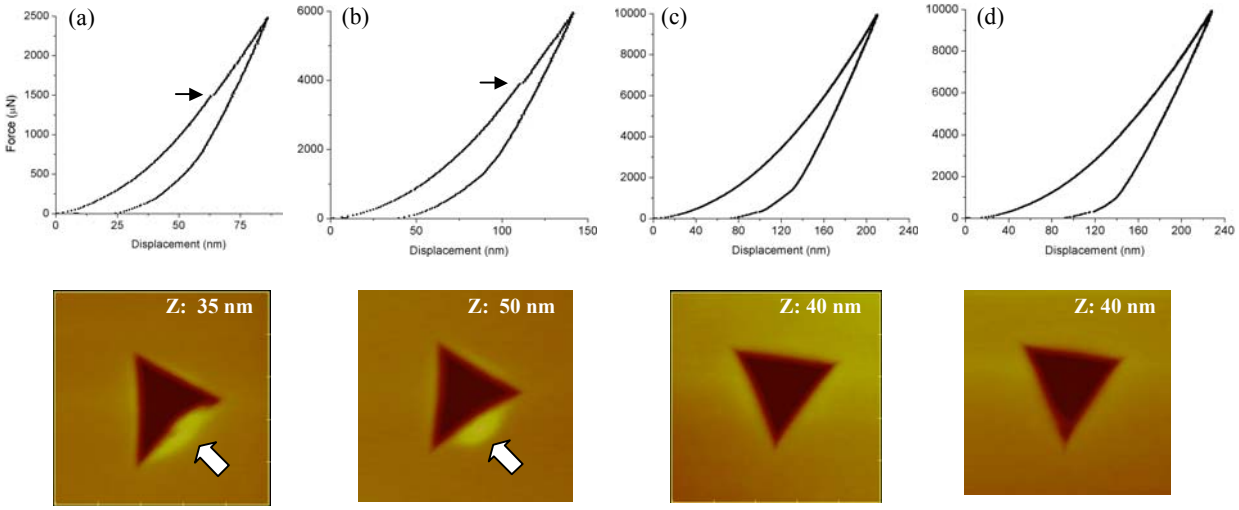

Figure 1. Indentation curves (load vs. displacement) and corresponding post AFM images for SiO_2 films thermally grown on Si at 1000˚C for the duration of a) 100 sec; b) 1,000 sec; c) 10,000 sec; d) 100,000 sec. The arrows indicate the pop-in event that can be related to buckling of the films as shown in AFM. Scan sizes are 2.5 x 2.5 μm, and z-scan range is given in each AFM image.

A pop-in effect is observed at about 1,600-μN load and 63-nm indentation depth for the former oxide film, whereas the same effect is observed at around 4,000-μN load and 110-nm indentation depth for the latter film, as shown in Fig. 1a and b. However, the two thicker films display no indication of the pop-in effect as shown in Fig. 1c and d. It indicates that the pop-in event should be related to the thickness of the thermal oxide films. The films that have the pop-in effect indeed displayed pile-up on the surface around the indented area as shown in the AFM images. This can be related to the buckling of the film after the interfacial delamination.

Figure 2 shows the effect of indentation depth on elastic modulus of the SiO_2 films on Si along with that of a single crystal Si. All five materials show a lower elastic modulus at very shallow depths, due to overestimation of the indented area at low forces typical for the brittle, elastic materials [18]. It becomes almost constant as the indentation depth increases to ≈ 100 nm. In this constant modulus regime, the first two SiO_2 films (100 and 1,000-sec annealing) exhibit elastic modulus very close to that of bare Si, indicating the substrate effect from the stiffer Si. On the other hand, the last two SiO_2 films (10,000 and 100,000-sec annealing) show lower elastic modulus as the indentation is made far away from the Si substrate.

Hardness values are also compared at different indentation depths for bare Si and four SiO_2 films as shown in Fig. 2b. The aforementioned surface artifact can also be found at shallow depths, and again, after ≈ 100 nm, the hardness becomes less sensitive to the indentation depth. Unlike the modulus data, there is no significant difference in hardness among the films. The hardness values are also close to those of Si. In particular, Si shows a decreasing trend in hardness with indentation depth at higher loads (e.g., > 5,000 μN) [18]. For the 10,000 and

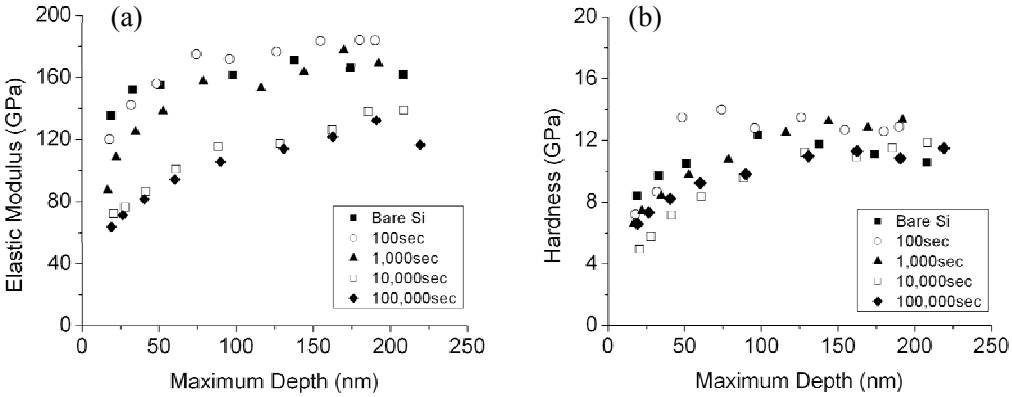

Figure 2. Effect of indentation depth on (a) elastic modulus, and (b) hardness of SiO_2 films grown on Si. For comparison, Si modulus and hardness are also shown in the figure.

100,000-sec annealed films, there is a much lesser substrate effect for hardness that gives a closer value to 'true' hardness of the SiO_2 films.

Saha and Nix [16] modified the analytical model proposed by King [19] to assess the influence of substrate modulus on the measured film modulus. This model was also adjusted to a three-sided pyramidal Berkovich indenter. The following relation was derived.

$$\frac{1}{E_r} = \frac{1-\nu_i^2}{E_i} + \frac{1-\nu_f^2}{E_f}\left(1 - e^{-\frac{\alpha(t-h)}{a}}\right) + \frac{1-\nu_s^2}{E_s}\left(e^{-\frac{\alpha(t-h)}{a}}\right) \quad , \qquad (6)$$

where subscripts i, f, and s represent indenter, film and substrate respectively, a is the square root of the projected contact area, t is the thickness of the film, h is the total indenter displacement, and α is a numerically determined scaling parameter that is a function of a/t and indenter geometries.

Figure 3 shows the results from this model by eliminating the substrate effect for the four SiO_2 films. An overall average for elastic modulus for the SiO_2 films was 86 ± 9.1 GPa. Elastic modulus values fall well within the average value, except for the last two data points that were annealed for 10,000 sec (h/t ≈ 0.68) and 100,000 sec (h/t ≈ 0.61). It seems that the above model for 'film-only' modulus (E_f) may not work well for the indentation depth beyond ≈ 60 % of the film thickness.

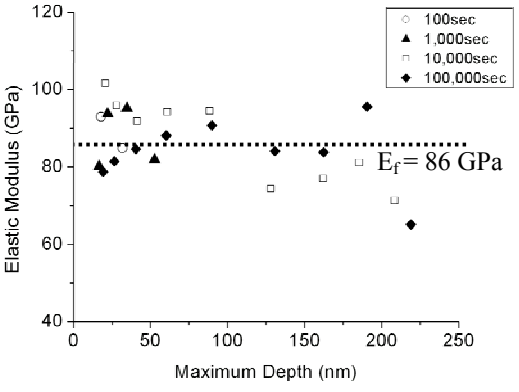

Figure.3. Corrected elastic modulus of SiO_2 films via the model by Saha and Nix. Note that the average film modulus was 86 GPa.

The average hardness values for four different films are shown in Fig. 4. A reasonable depth range was *manually* picked so that the hardness can be kept from both surface and substrate effects. But as shown, it is difficult to avoid the substrate effect for very thin films. The hardness values display a slightly lower value (8.7 GPa) for the 100-sec annealed films as compared to the other longer annealed films that show more consistent values (9.6 - 11.1 GPa). The first two shorter annealed films (100 and 1,000 sec) displayed a larger substrate effect (the difference in hardness values).

While working on the substrate effect on the film modulus, we explored using P/S^2. For this purpose, hardness values selected from Fig. 4 (film-only) were used for each film. Although the hardness of the film must be determined from the elastically homogeneous materials to utilize P/S^2, it is deemed acceptable here, considering that we are mainly interested in isolating the substrate effect [16]. The corrected E_r and A were then calculated by Eq. (4) and Eq. (5), respectively, for each indentation. Using these two parameters, Eq. (6) can be used to obtain the 'true' film modulus by subtracting the substrate effect (Fig. 5). The elastic modulus values of the films show no dependence on the film thickness, hovering around 88 GPa, similar to the one obtained in Fig. 3. It is clearly seen that raw modulus data (with the substrate effect) have been overestimated for all four films, among which the largest substrate effect is observed at the thinnest film (100 sec) (Fig. 5).

In addition, the above model can be used to estimate thin film thickness if elastic properties of the substrate are known [17]. For example, with known film modulus, an inverse analysis can be performed to deduce the film thickness. In this analysis, the film thickness can be expressed as a function of a parameter x which contains elastic properties of diamond indenter, film and substrate:

$$t = h - \frac{a_c}{\alpha}\ln(x) \quad . \tag{7}$$

The scaling parameter α in the above equation also depends on t and a_c. As a result, thickness, t in Eq. (7) can be obtained via numerical methods. In fact, the inverse analysis was performed on the 100,000-sec annealed SiO_2 film (370-nm thick film from ellipsometry measurement), and the estimated thickness was about 398 nm.

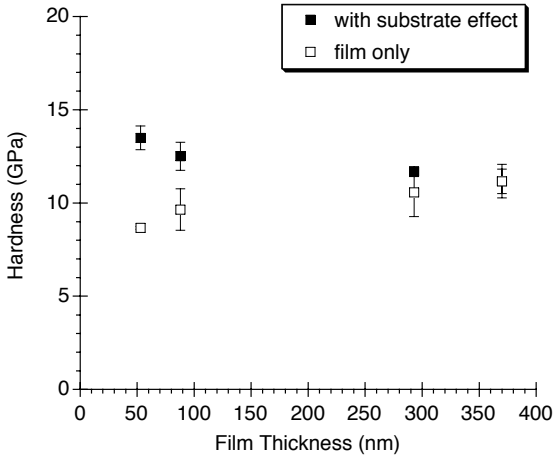

Figure 4. Hardness of different thickness of SiO_2 films. Film-only hardness values were manually picked from experimental data.

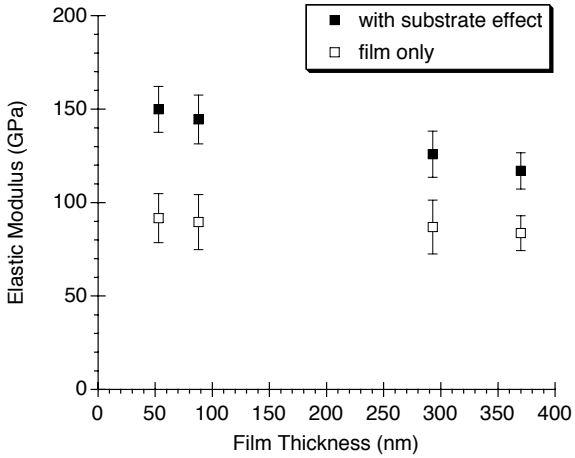

Figure 5. Elastic modulus of different thickness of SiO_2 films. Film-only modulus values were modeled through Eq. (6).

CONCLUSIONS

In this work, we investigated mechanical properties of thermally grown SiO_2 films on Si through nanoindentation. There existed a pop-in effect for very thin films in the loading curve, which could be related to the buckling of the oxide films due to the interfacial delamination. The substrate effect has been isolated via the model by Saha and Nix to deduce the 'film-only'

mechanical properties. It was observed that elastic deformation is more influenced by the presence of the substrate than plastic deformation. In particular, the SiO_2 film modulus of ≈ 88 GPa was obtained assuming a constant hardness value for each film (ranging from 8.7 to 11.1GPa). The hardness values were slightly lower for very thin SiO_2 film, whereas the modulus values were almost constant with the film thickness. The estimation of the film thickness via an inverse analysis from the same model agreed well with the experimental ellipsometry measurements. This study is expected to shed a light on the mechanical behavior of thin films at small scales, and to provide a means to estimate the true film properties while eliminating the substrate effect. More work is, however, needed to apply the current model to a high ratio of the indentation depth to the film thickness.

ACKNOWLEDGMENTS

This work was funded by Infotonics Technology Center, Inc. (NASA Grant #: NAG3-2744). The authors would also like to thank Prof. X. Wang and Mr. Y. Liu for helping with ellipsometry measurements.

REFERENCES

1. X. Li, D. Diao, B. Bhushan, *Acta Mater.*, **45**, 4453-4461 (1997).
2. Y. Choi and S. Suresh, *Acta Mater.* **50**, 1881-1893 (2002).
3. N.R. Moody, D. Medlin, D. Boehme, D.P. Norwood, *Eng. Frac. Mech.*, **61**, 107-118 (1998).
4. M.F. Doerner and W.D. Nix, *J. Mater. Res.*, **1**, 601 (1986).
5. P. Balk, *Adv. Mater.,* **7**, 703 (1995).
6. D.L. Griscom, *MRS Bull.*, Jun-Aug 20 (1987).
7. W. Kern and R.S. Rosler, *J. Vac. Sci. Technol.*, **14**, 1082 (1977).
8. S.A. Campell, *The Science and Engineering of Microelectronic Fabrication*, Oxford University Press, (1996).
9. L. Pitchon, K. Mourgues, F. Raoult, T. Mohammed-Brahim, K. Kis-Sion, D. Briand, O. Bonnaud, *Semicond. Sci. Technol.*, **16**, 918 (2001).
10. G. Hass and N.W.Scott, *J. Opt. Soc. Am.*, **39**, 179 (1949).
11. J.A. Savage, *Infrared Optical Materials and their Antireflection Coatings*, Adam Hilger Ltd., Bristol (1985).
12. I-Fan Wu, J.B. Dottellis, and M. Dagenais, *J. Vac. Sci. Technol. A*, **11,** 2398 (1993).
13. K. Saito, Y. Uchiyama, and K. Abe, *Thin Solid Films*, **430**, 287 (2003).
14. G.M. Pharr and W.C. Oliver, *MRS Bull.*, XVII (7) 28 (1992).
15. D.L. Joslin and W.C. Oliver, *J. Mater. Res.*, **5**, 123 (1990).
16. R. Saha and W.D. Nix, *Acta Mater.*, **50**, 23 (2002).
17. W.C. Oliver and G.M. Pharr, *J. Mater. Res.*, **19**, 3 (2004).
18. F. Helvaci, *M.S. Thesis*, SUNY Binghamton (2004).
19. R.B. King, *Int. J. Solids Struct.*, **23**, 1657 (1987).